ガモフ･テラー遷移
と宇宙物理における弱い相互作用

笹野　匡紀
上坂スピン･アイソスピン研究室
理研仁科加速器センター

ガモフ・テラー遷移と荷電交換反応

ガモフ・テラー(GT)遷移

$\Delta T=1, \Delta S=1, \Delta L=0$

$\vec{\sigma}\, t_{\pm}$

強度：B(GT)

→ **許容β崩壊**

中間エネルギーの荷電交換反応

e.g. (p,n), (3He,t), (d,2He), ….

$$\left(\frac{d\sigma}{d\Omega}(q=0)\right)_{(p,n)} = \hat{\sigma}\, B(GT)$$

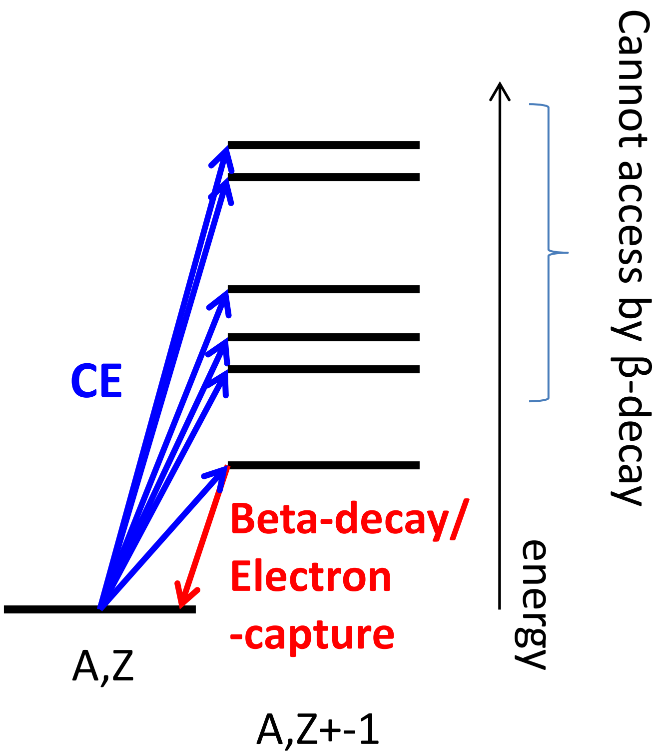

荷電交換反応の応用

Possible to probe
any Ex on any A/Z

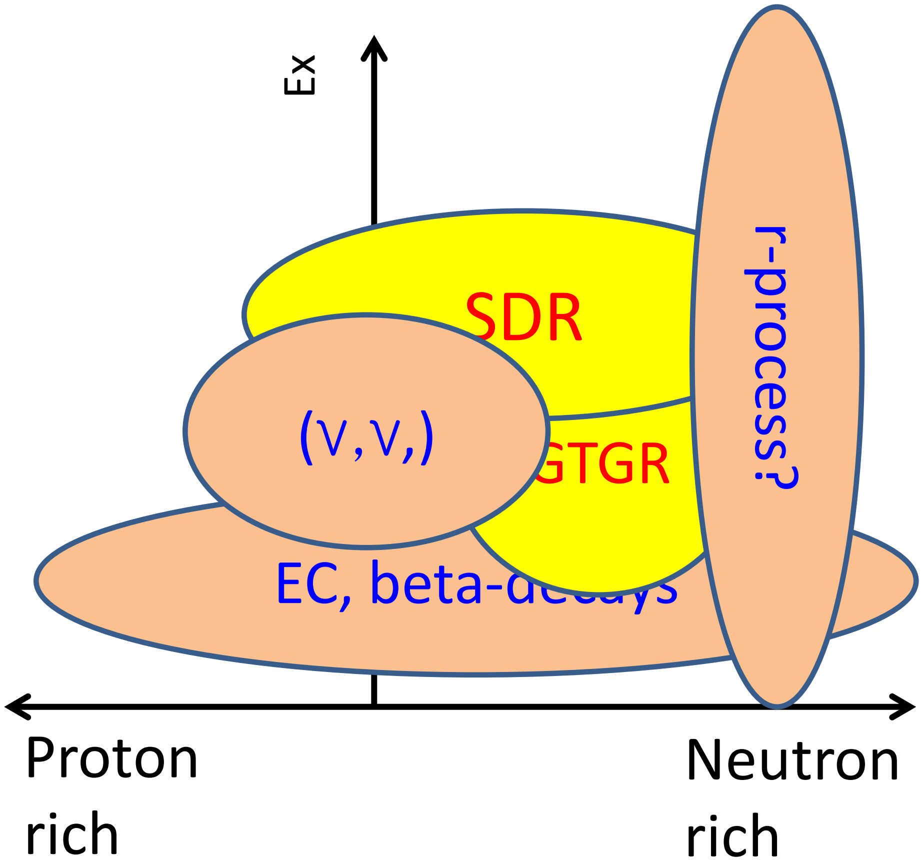

^{6}He, ^{11}Li, ^{14}Be,
$^{70,72}Ni$, ^{132}Sn
at RIKEN RIBF

- GTGR, SDR
- EC/beta-decays
- Neutral weak currents,

  e.g., Synthesis of Mn in Poplution III star
  $^{56}Ni(\nu,\nu p)^{55}Co \rightarrow {}^{55}Fe \rightarrow {}^{55}Mn$
  GXPF1 >> KB3G (a factor of 3)
  T. Suzuki et al., Phys. Rev. C79, 061603(R) (2009).
- R-process (GT + first forbidden)

T. Suzuki et al., arXiv:1110.3886

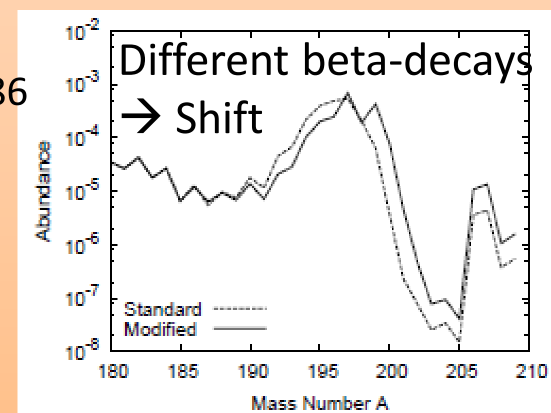

電子捕獲

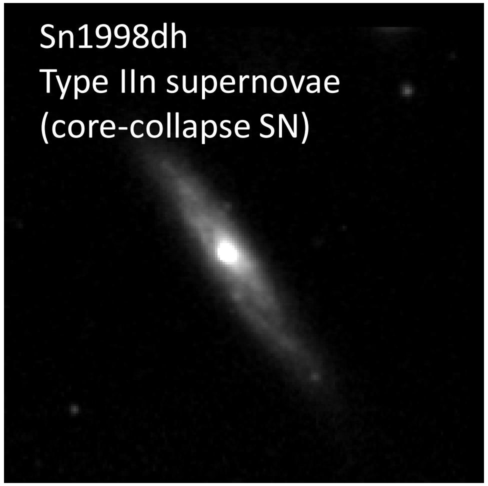

Core-Collapse (Type II) Supernovae

- Collapse of massive star at the end of burning cycle electron-capture (EC) on Fe-region nuclei
- reduces electron pressure
- neutrinos by EC carry away energy from the star → collapse accelerates
- affects the mass interior to the shockwave

Thermonuclear (Type Ia) Supernovae

- source of large fraction of Iron group nuclei in the universe
- thermonuclear explosions of accreting white dwarfs in binary systems **Not well understood.**

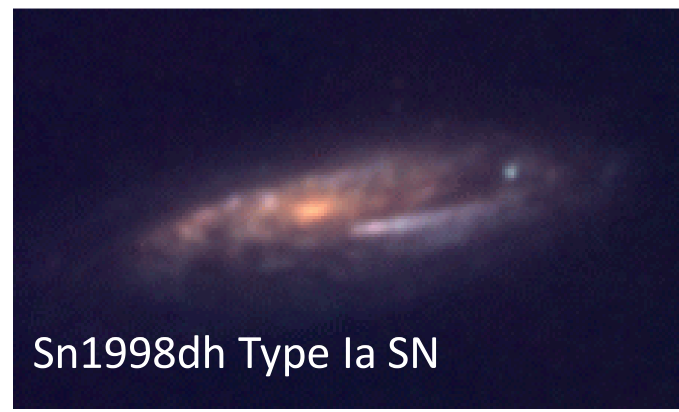

- ECs strongly affect the flame propagation after ignition
- If ECs are well understood → models can be much better constrained

Key : 鉄領域における電子捕獲

超新星爆発におけるガモフ·テラー遷移

- Key ingredient: **Gamow-Teller strengths**
- Many nuclei play a role (A-40-120)
- Majority are unstable
- excitation can take place from excited nuclear states

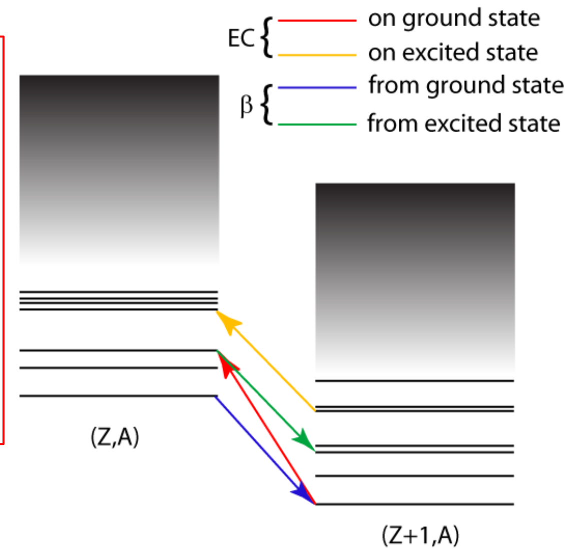

Impossible to measure even a sizeable fraction of cases

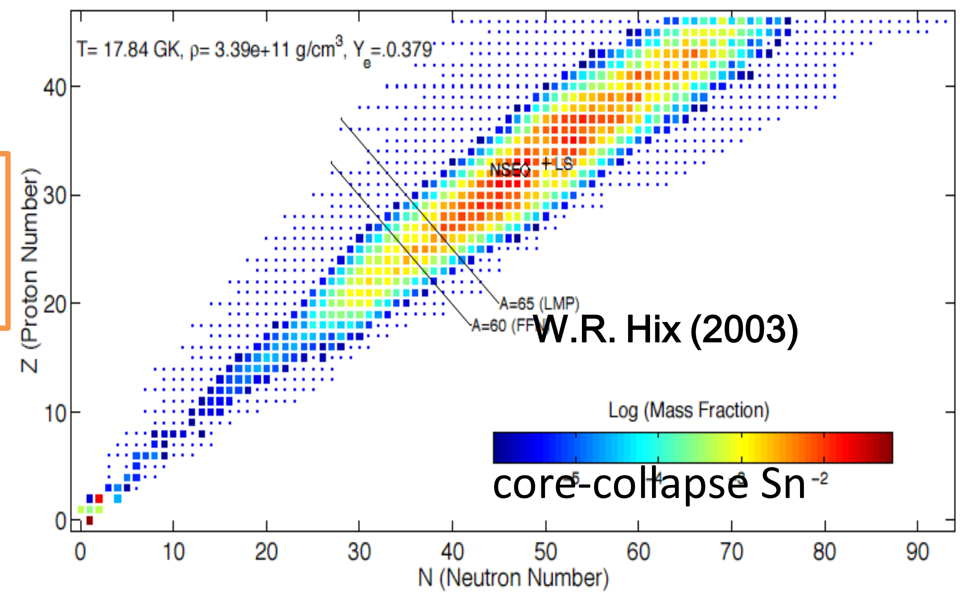

戦略…

キーとなる原子核（二重閉殻核、興味のある宇宙物理現象で豊富な核）をはかる。

→背後にある物理を明らかにする（相互作用、配位混合、。。。。）

→核モデルを向上

→弱い相互作用反応率核モデルの予言能力を向上

^{56}Niの電子捕獲

One of the important cases

in core collapse super novae of massive stars

(Phys. Rev. Lett. 86, 1678 (2001))

TABLE I. Most important nuclei for electron capture and beta decay at selected points (characterized by temperature T, density ρ, and electron-to-baryon ratio Y_e) during the final evolution of $15M_\odot$ and $25M_\odot$ stars. The total electron capture λ_{ec} and beta decay λ_{β^-} rates are listed as well as the 3 dominating nuclei; the number in parentheses defines their percentage to the respective rates.

T (K)	ρ (g cm^{-3})	Y_e	λ_{ec} (s^{-1})	Electron capture			λ_{β^-} (s^{-1})	Beta decay		
					$15M_\odot$					
3.39×10^9	4.50×10^7	0.480	5.17×10^{-7}	^{54}Fe (29)	^{55}Fe (25)	^{53}Mn (11)	6.08×10^{-11}	^{54}Mn (67)	^{55}Mn (8)	^{32}P (7)
3.82×10^9	7.26×10^7	0.464	3.30×10^{-7}	^{55}Fe (41)	^{57}Co (10)	^{53}Mn (9)	6.73×10^{-9}	^{56}Mn (45)	^{60}Co (18)	^{55}Mn (11)
4.13×10^9	2.89×10^8	0.450	6.86×10^{-7}	^{57}Fe (54)	^{61}Ni (21)	^{56}Fe (14)	4.10×10^{-7}	^{56}Mn (36)	^{52}V (12)	^{57}Mn (10)
4.41×10^9	1.30×10^9	0.442	7.57×10^{-6}	^{57}Fe (22)	^{53}Cr (14)	^{55}Mn (13)	1.74×10^{-6}	^{58}Mn (34)	^{62}Co (17)	^{64}Co (12)
7.25×10^9	9.36×10^9	0.432	9.21×10^{-3}	^{65}Ni (14)	^{59}Fe (7)	^{52}V (7)	8.45×10^{-6}	^{64}Co (22)	^{58}Mn (19)	^{54}V (13)
					$25M_\odot$					
3.79×10^9	2.89×10^7	0.487	3.18×10^{-6}	^{53}Fe (23)	^{55}Co (20)	^{56}Ni (19)	1.53×10^{-11}	^{54}Mn (49)	^{55}Fe (17)	^{58}Co (9)
4.17×10^9	3.71×10^7	0.476	4.23×10^{-6}	^{54}Fe (21)	^{55}Co (14)	^{55}Fe (11)	8.12×10^{-10}	^{54}Mn (37)	^{58}Co (30)	^{55}Fe (8)
5.03×10^9	1.82×10^8	0.456	3.84×10^{-6}	^{56}Fe (17)	^{55}Fe (13)	^{61}Ni (10)	1.00×10^{-6}	^{56}Mn (45)	^{52}V (13)	^{60}Co (10)
5.57×10^9	5.05×10^8	0.449	1.45×10^{-5}	^{57}Fe (16)	^{56}Fe (11)	^{53}Cr (9)	7.61×10^{-6}	^{56}Mn (19)	^{58}Mn (14)	^{55}Cr (10)
7.75×10^9	2.42×10^9	0.445	1.95×10^{-3}	^{1}H (32)	^{53}Cr (9)	^{57}Fe (7)	5.17×10^{-5}	^{58}Mn (18)	^{55}Cr (13)	^{57}Mn (7)

^{56}Niにおける電子捕獲と(p,n)反応

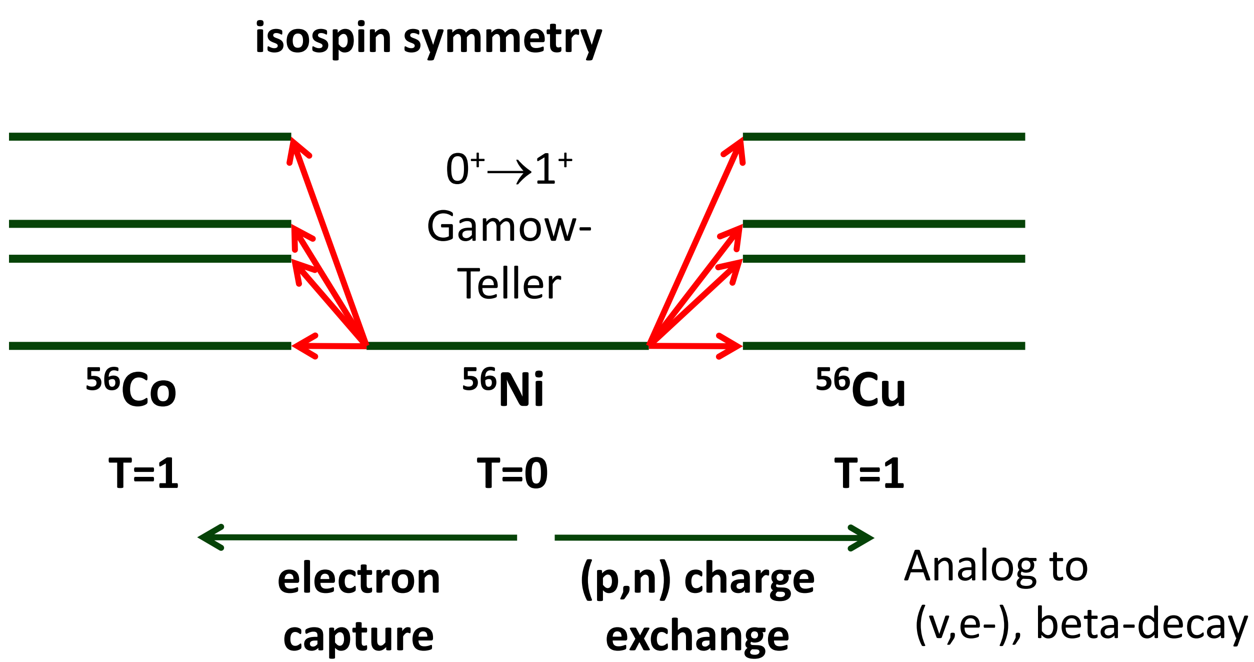

B(GT) measured by the (p,n) reaction is directly connected with the EC rate.

^{56}Ni はキーとなる核

^{56}Ni (Z=N=28)

- independent particle model
  → ^{56}Ni is doubly magic
- Large p-n residual interaction
  → ^{56}Ni is not magic

- **GT strength from ^{56}Ni**
  → key to bench mark nuclear model used for weak rates in the Fe region

Experimentally, challenging!

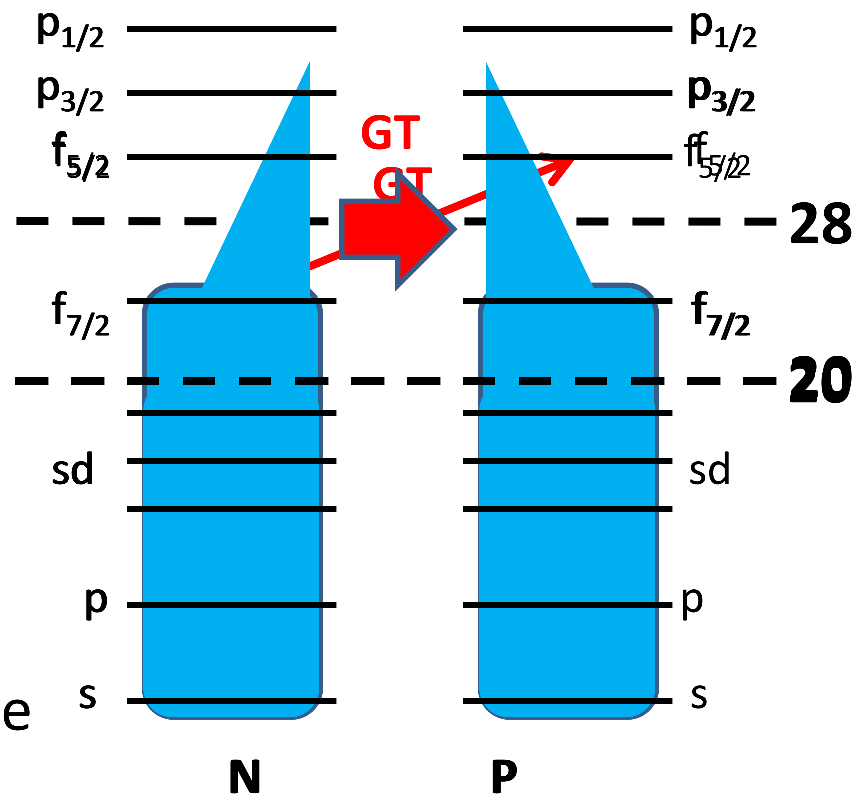

f7/2 70% in ^{56}Ni (GXPF1A, KB3G)
(e.g., Honma et al., Phys. Rev. C 69, 034335 (2004))

実験手法

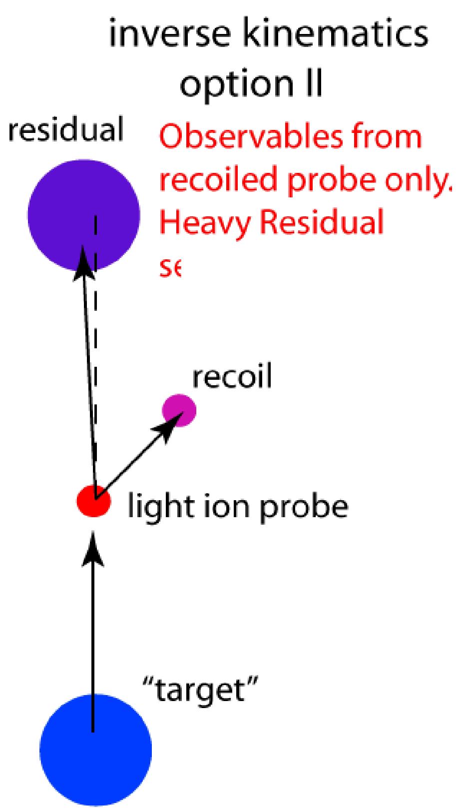

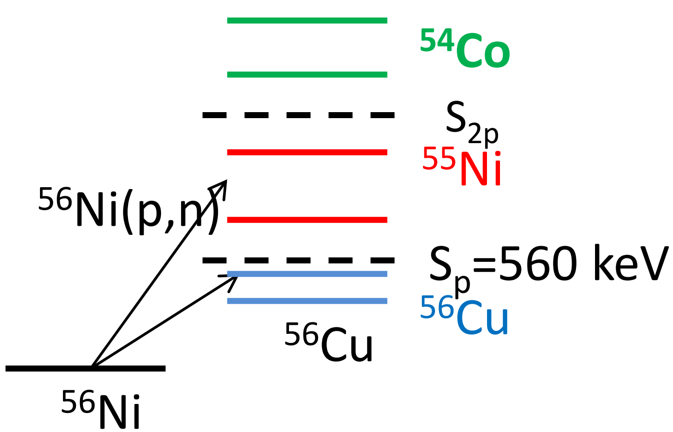

Missing mass spectroscopy by the detection of the recoil neutron

Advantages

- target can be thick (neutron recoil)
  → high luminosity
  even with unstable beams
  with low intensities

- All kinematic information from measurement of the neutron (two-body kinematics)
  → simple measurement and analysis,
  compared to invariant mass method

- Heavy fragment serves as tag for CE reaction
  → branching ratio of the particle decay

Can be applied to any mass region and to any excitation energy

^{56}Ni ビーム生成とセットアップ

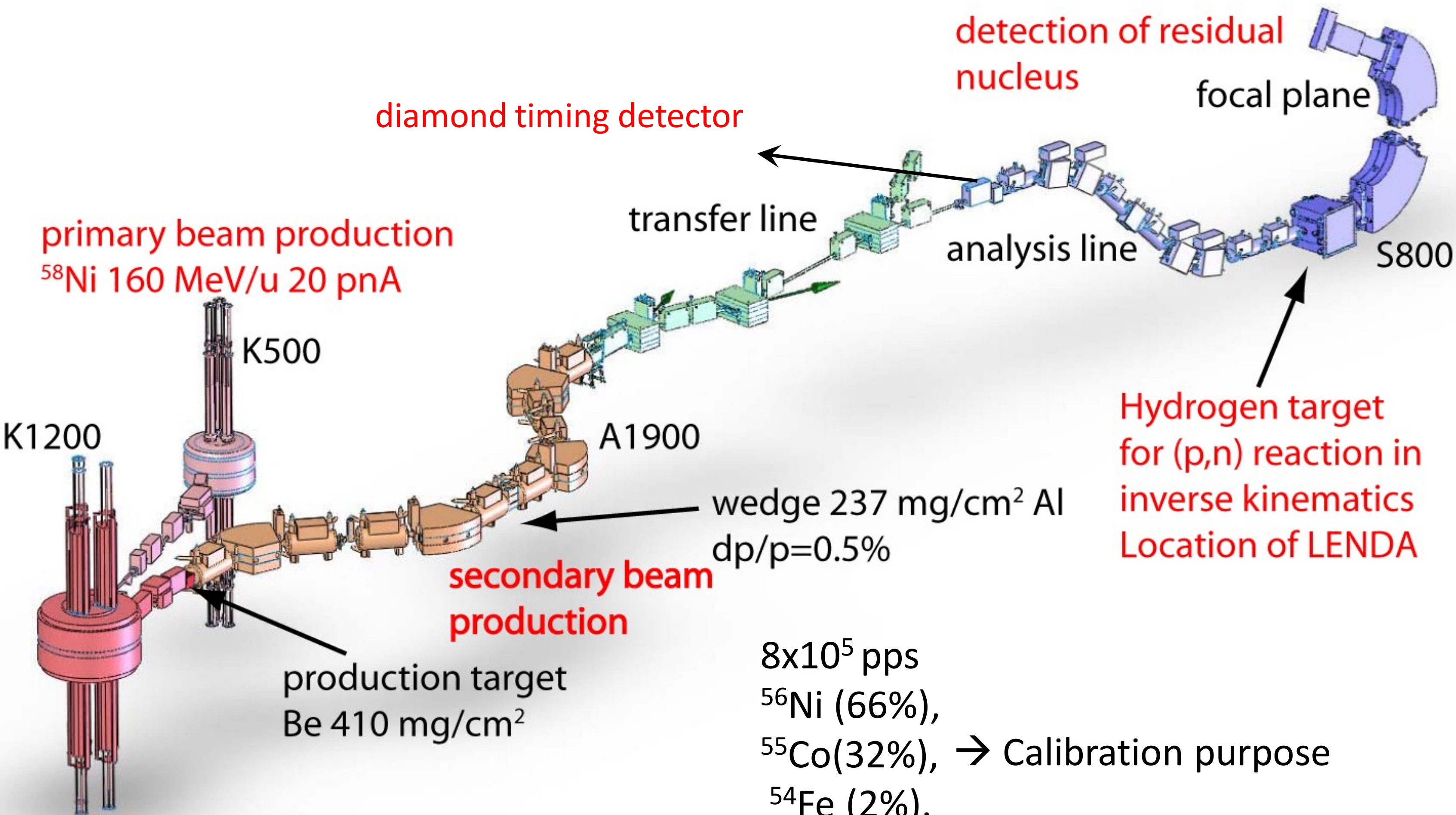

8×10^5 pps
^{56}Ni (66%),
^{55}Co(32%), → Calibration purpose
^{54}Fe (2%).

National Superconducting Cyclotron Laboratory,
Michigan State University

LENDAのセットアップ

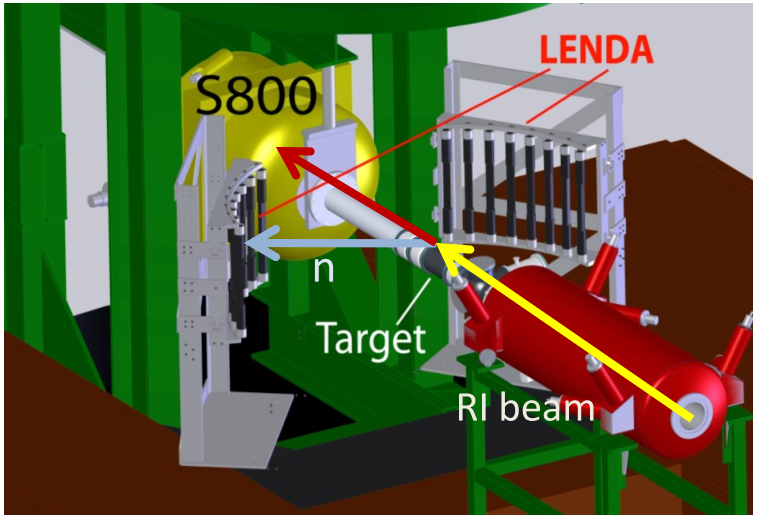

Low Energy Neutron Detector Array (LENDA)
neutron detection
Plastic scintillator
24 bars 2.5x4.5x30cm
150 keV < E_n < 10 MeV
ΔE_n ~ 5% $\Delta\theta_n < 2^o$
efficiency 15-40%
Flight path : 1 m

Neutron energy & angles

Excitation energy
& reaction scattering angles

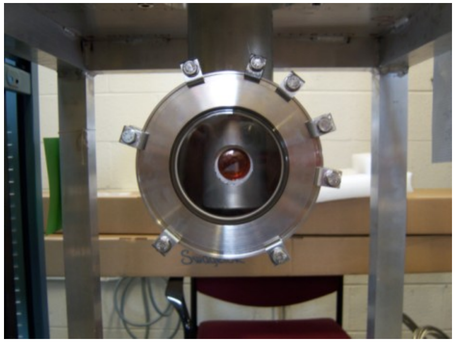

Liquid Hydrogen target
"proton " target
65 mg/cm^2 (~7 mm)
~3.5 cm diameter
T=20 K ~1 atm

結果

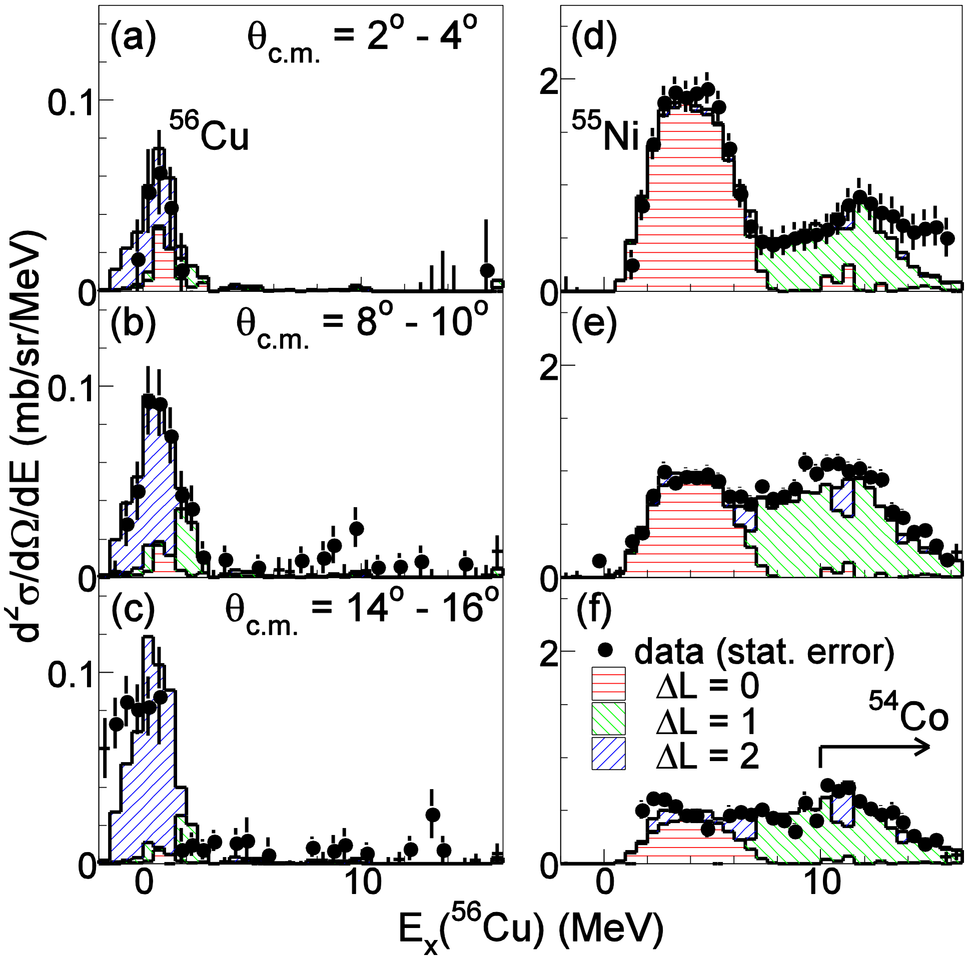

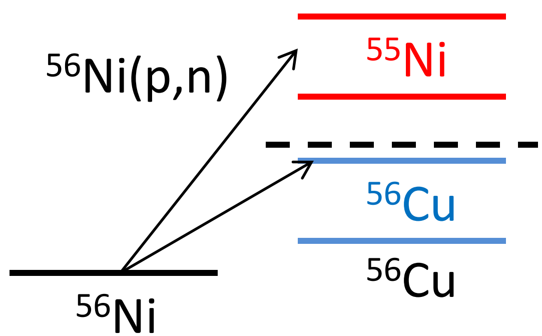

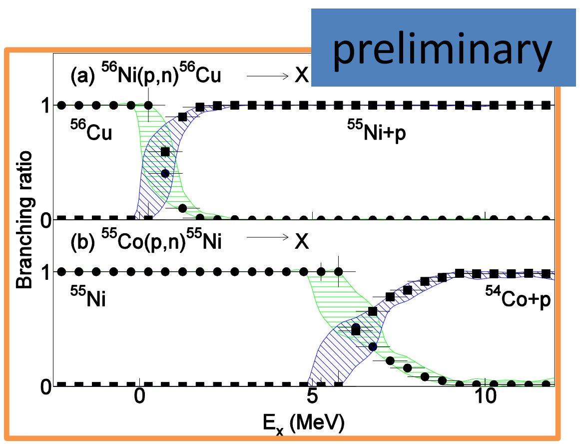

GTR and SDR are extracted!

^{56}Niのガモフ・テラー強度

- Use the extracted ΔL=0 component in combination with unit cross section to extract Gamow-Teller strength [B(GT)].
- Compare with large-scale shell-model calculations

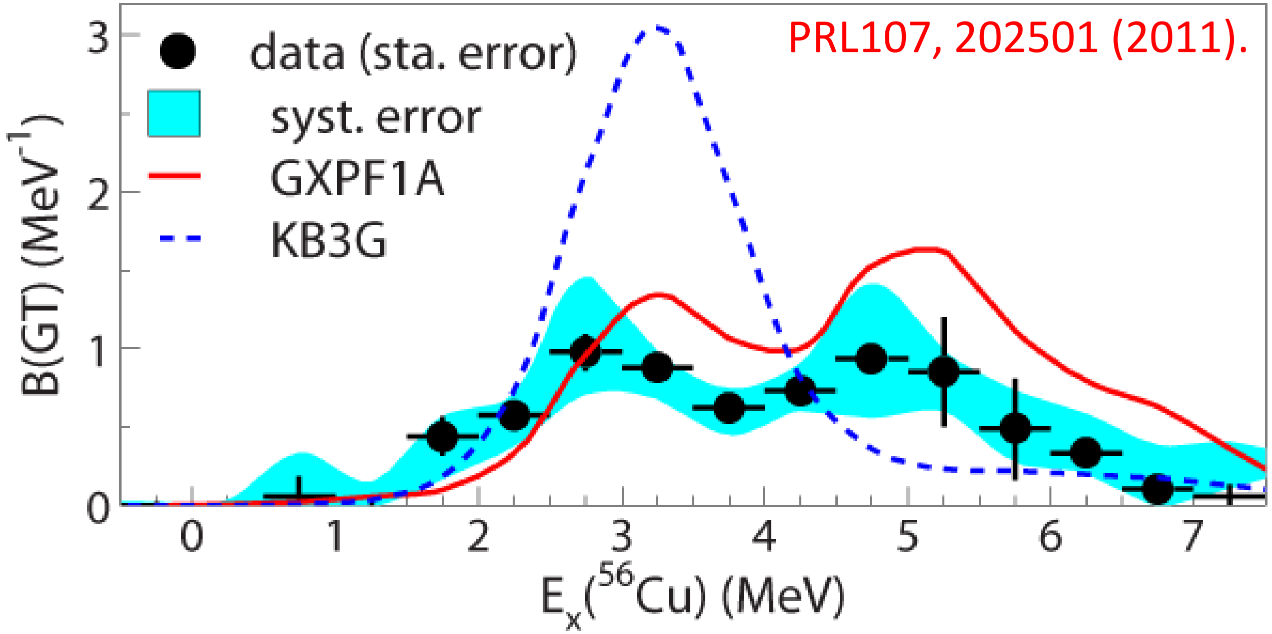

GXPF1A: Honma et al. : constrained by data in full pf-shell

KB3G: Poves et al. : less constraints – used in database for weak rates for astrophysical purposes.

Difference between KB3G and GXPF1A:

- KB3G weaker spin-orbit and pn-residual interactions
- KB3G lower level density

^{55}Coのガモフ･テラー強度

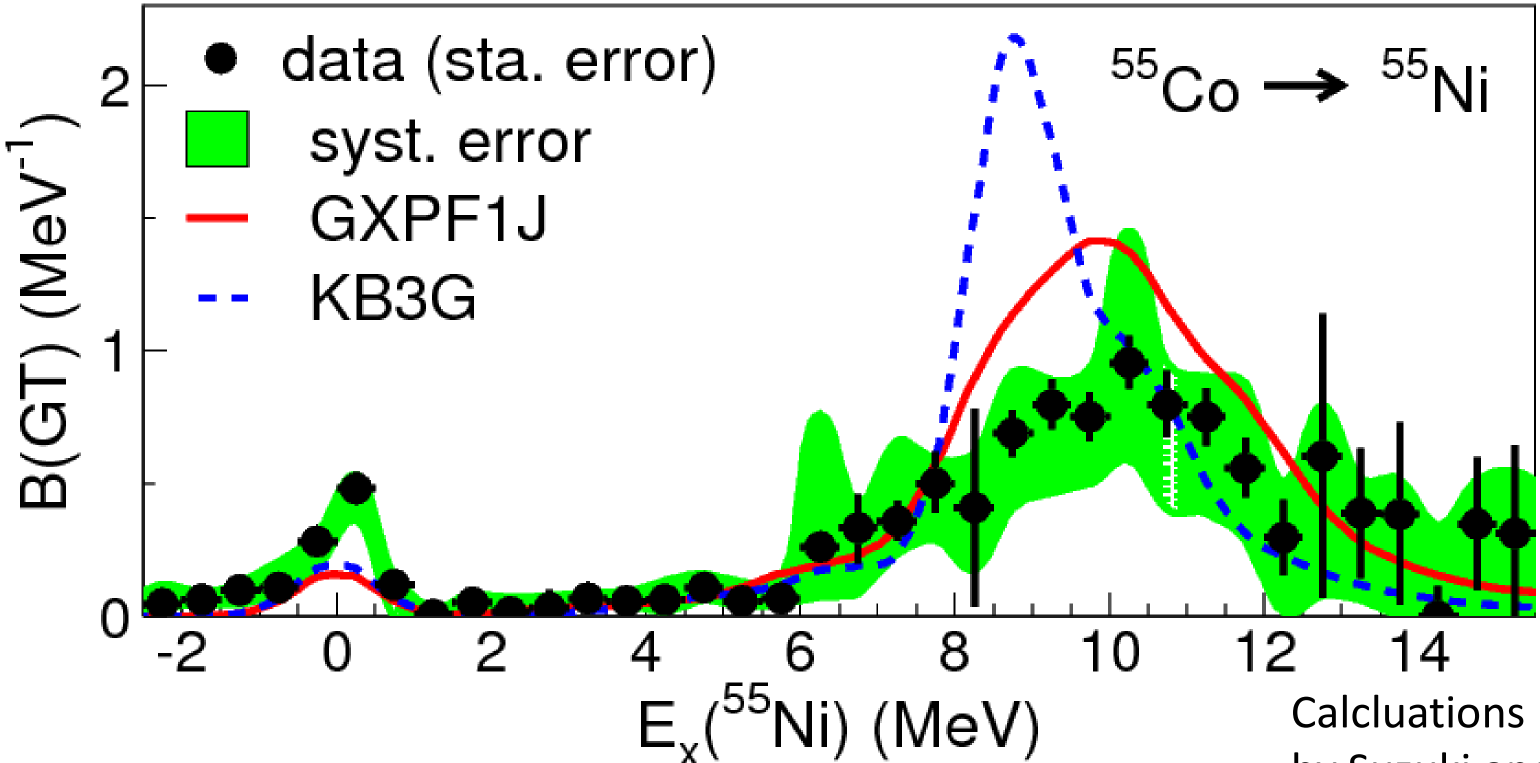

Calcluations
by Suzuki and Honma

KB3G : X

GXPF1”J” : O

Consistent with the comparison in ^{56}Ni

核構造の物理

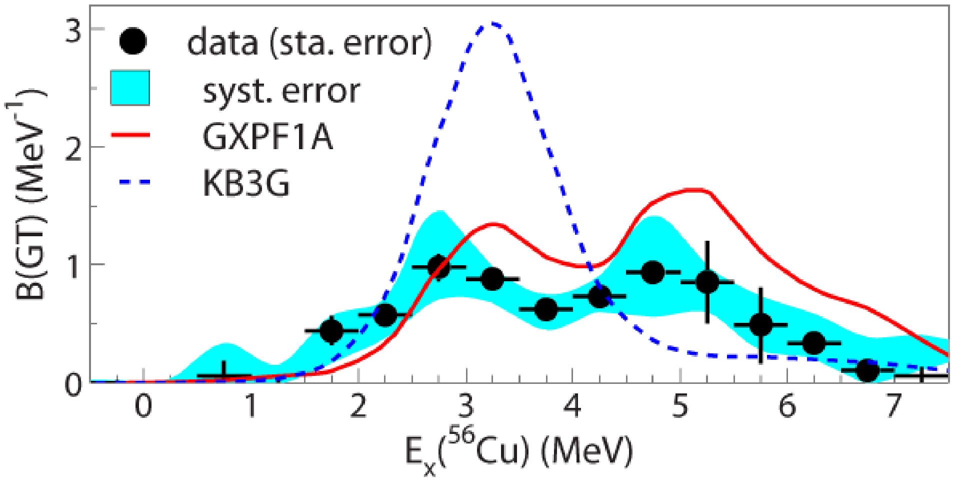

Two prominent peaks exist
Large difference between KB3G and GXPF1

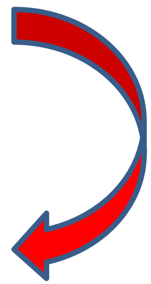

Remove one neutron
from parent & daughter

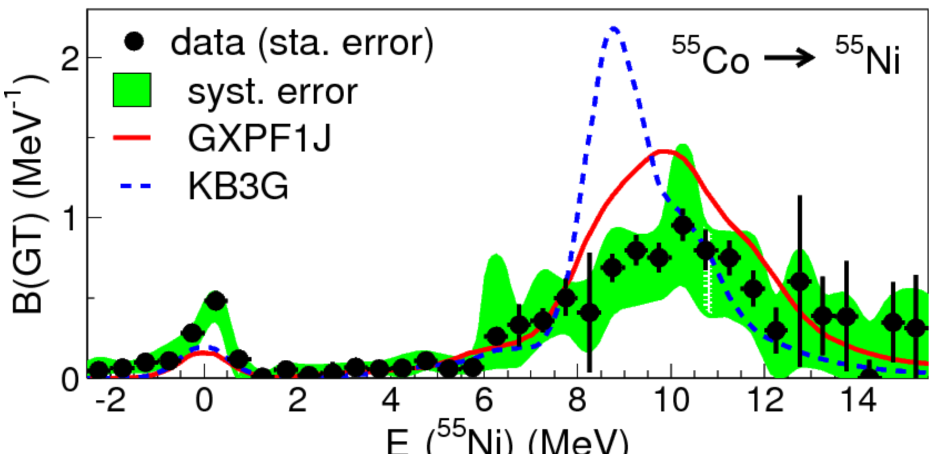

Two peaks disappear
Small difference between KB3G and GXPF1

Point:
Along N=Z, B(GT) is sensitive to some part of interaction and showing two peaks.
Question:
What picture can **intuitively** explain the origin of the two peaks?

新しいガモフ·テラー共鳴？

(C. L. Bai, H. Sagawa, et al., Phys. Lett. B 719)

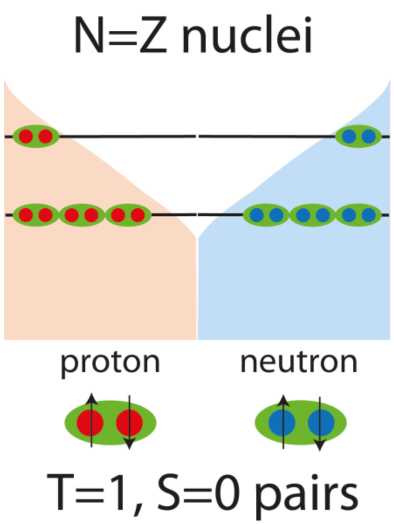

<u>Initial ground state</u>

Filled with pp/nn (isovector) pair

<u>GT transition</u>

breaking a pair

<u>Final state</u>

- **particle-hole**: repulsive
  → pushed up to higher energy
  (well studied in stable nuclei)
- **particle-particle (pn)**: attractive
  → pushed down to lower energy

The states in the lower peak is expected to form a T=0, S=1 pair (identical proton and neutron orbits)

最近の藤田佳孝（阪大理）氏の仕事 @RCNP

PRL 112, 112502 (2014) PHYSICAL REVIEW LETTERS week ending 21 MARCH 2014

Observation of Low- and High-Energy Gamow-Teller Phonon Excitations in Nuclei

Y. Fujita,[1,2,†] H. Fujita,[1] T. Adachi,[1] C. L. Bai,[3] A. Algora,[4,5] G. P. A. Berg,[6] P. von Brentano,[7] G. Colò,[8] M. Csatlós,[5] J. M. Deaven,[9] E. Estevez-Aguado,[4] C. Fransen,[7] D. De Frenne,[10,*] K. Fujita,[1] E. Ganioğlu,[11] C. J. Guess,[9,‡] J. Gulyás,[5] K. Hatanaka,[1] K. Hirota,[1] M. Honma,[12] D. Ishikawa,[1] E. Jacobs,[10] A. Krasznahorkay,[5] H. Matsubara,[1,§] K. Matsuyanagi,[13,14] R. Meharchand,[9,‖] F. Molina,[4,¶] K. Muto,[15] K. Nakanishi,[1,**] A. Negret,[16] H. Okamura,[1,*] H. J. Ong,[1] T. Otsuka,[17] N. Pietralla,[7,††] G. Perdikakis,[9,18] L. Popescu,[19] B. Rubio,[4] H. Sagawa,[12,13] P. Sarriguren,[20] C. Scholl,[7,‡‡] Y. Shimbara,[21,§§] Y. Shimizu,[1,‖‖] G. Susoy,[11] T. Suzuki,[1] Y. Tameshige,[1] A. Tamii,[1] J. H. Thies,[22] M. Uchida,[1] T. Wakasa,[1,¶¶]

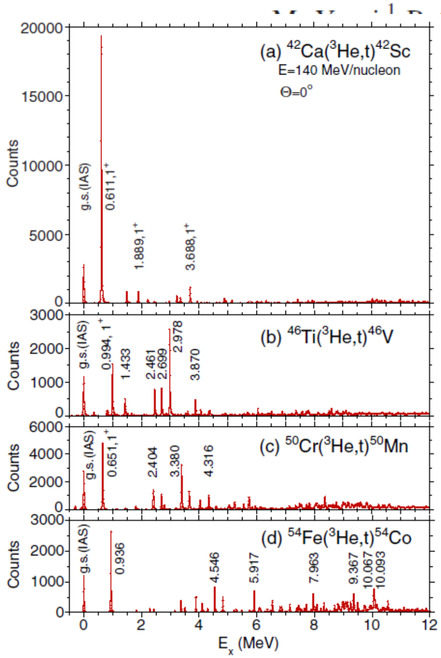

Also explained
by competition of p-h vs. p-p

理論をどう評価するか？
（MSUのグループの仕事）

A.L. Cole, R. G. T. Zegers et al., Phys. Rev. C 86, 015809 (2012)

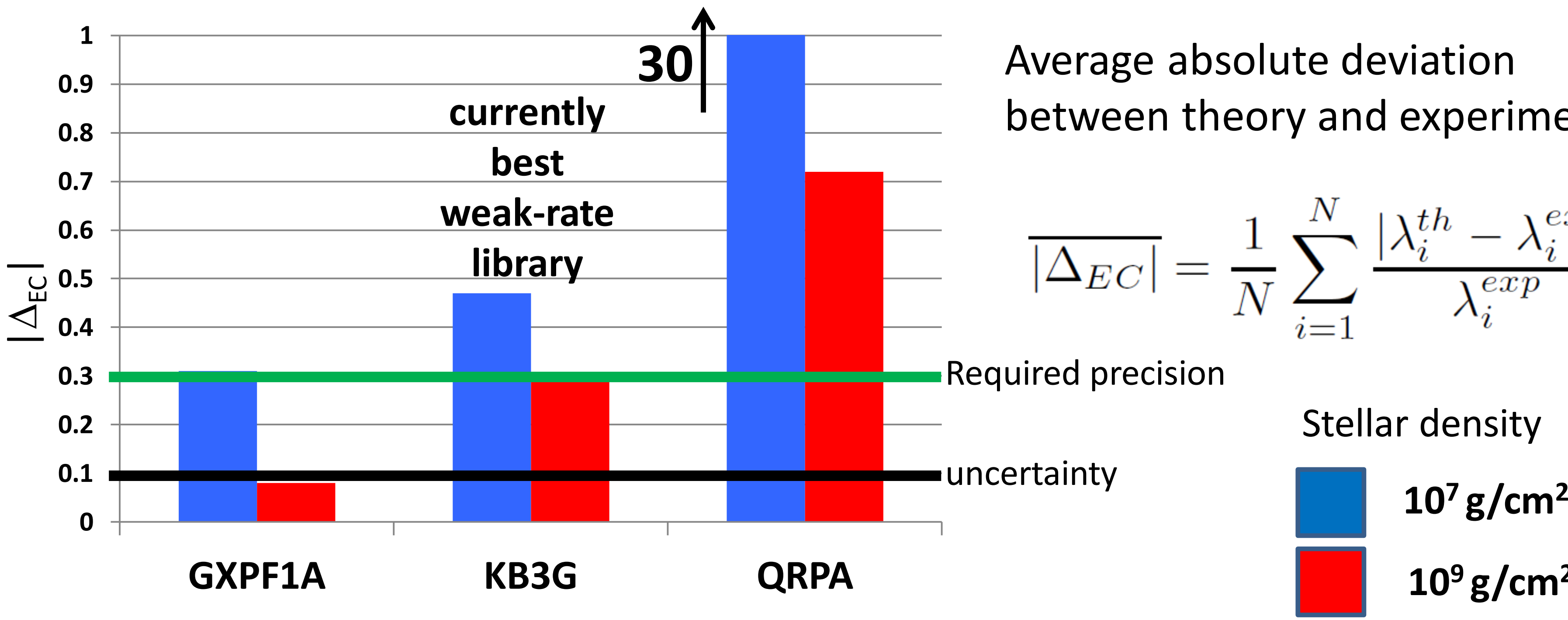

Average absolute deviation between theory and experiment

$$\overline{|\Delta_{EC}|} = \frac{1}{N}\sum_{i=1}^{N} \frac{|\lambda_i^{th} - \lambda_i^{exp}|}{\lambda_i^{exp}}$$

- systematic comparison of theory to charge-exchange data for stable pf-shell nuclei completed – except for lightest pf-shell nuclei
- preference for shell-model GXPF1A interaction - confirmed by ^{56}Ni(p,n) experiment
- relatively poor agreement for QRPA calculations

(p,n)反応プロジェクト@RIBF

RIKEN RIBF

Beam :

^{8}He, ^{11}Li, ^{14}Be, ^{70,72}Ni, ^{132}Sn at RIKEN RIBF
with enough intensity (> 10^4 pps)
with the best beam energy (200--300 MeV)
←→ NSCL cannot access neutron drip line

Neutron detection:

60 scintillator bars
←→24 bars

Residue tag :

Measure all decay particles in one setting
(No n-knockout/frag. background)
←→ only a part of decay particles

⇩

RIKEN RIBF is the most powerful facility for the (p,n) measurement in inverse kinematics
The first exp. at RIKEN for ^{12}Be by Yako et al.

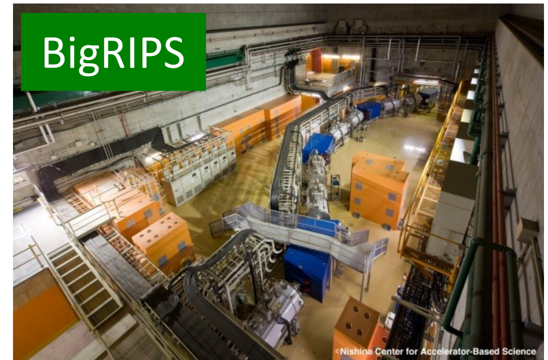

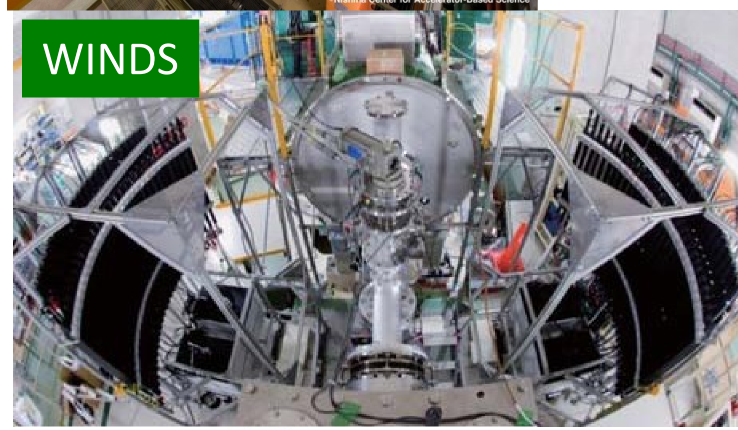

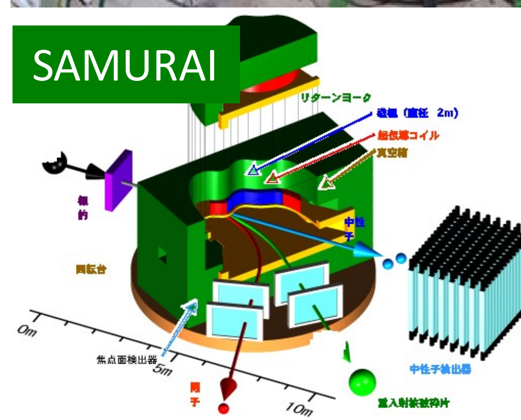

R過程への応用

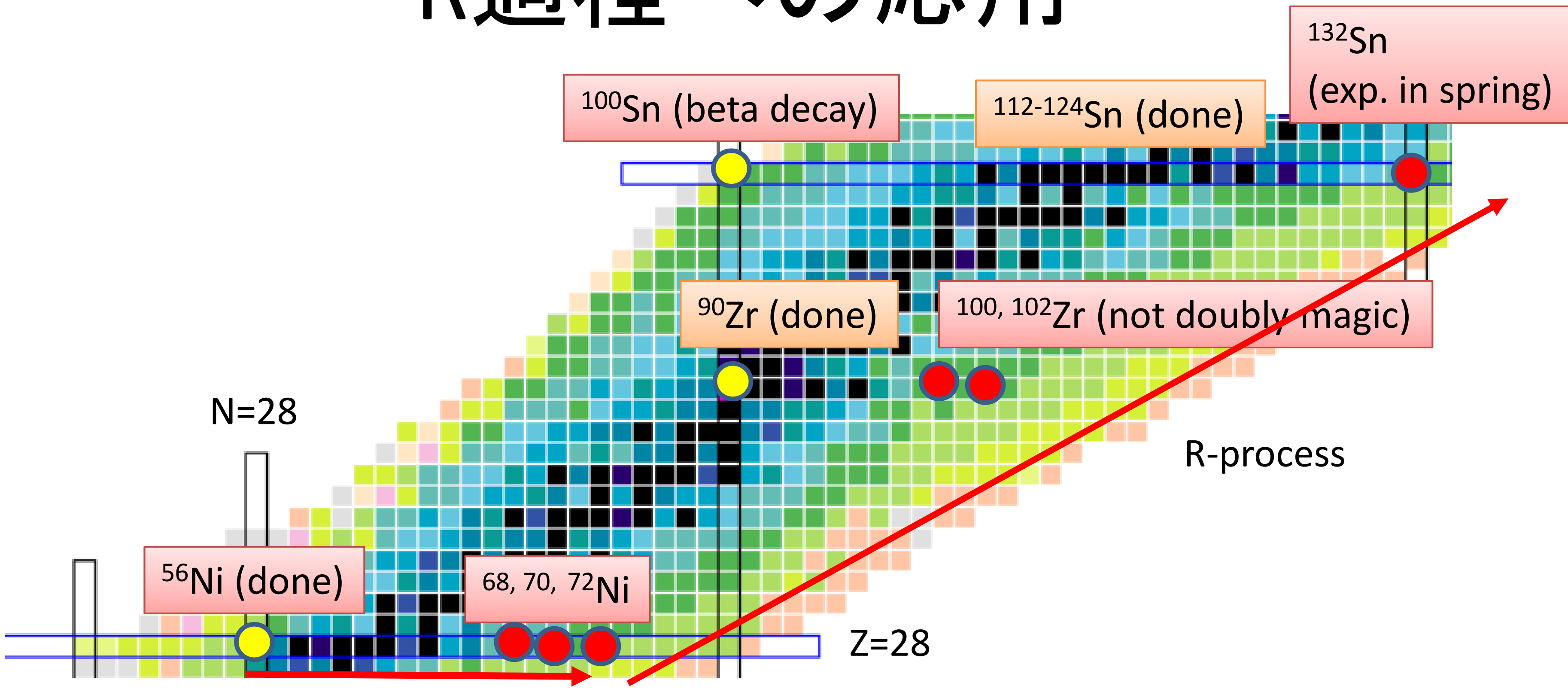

Measuring “key” nuclei
→ Benchmark calculations
→ Describe nuclear (beta-decay) processes in the r-process

rp過程への応用

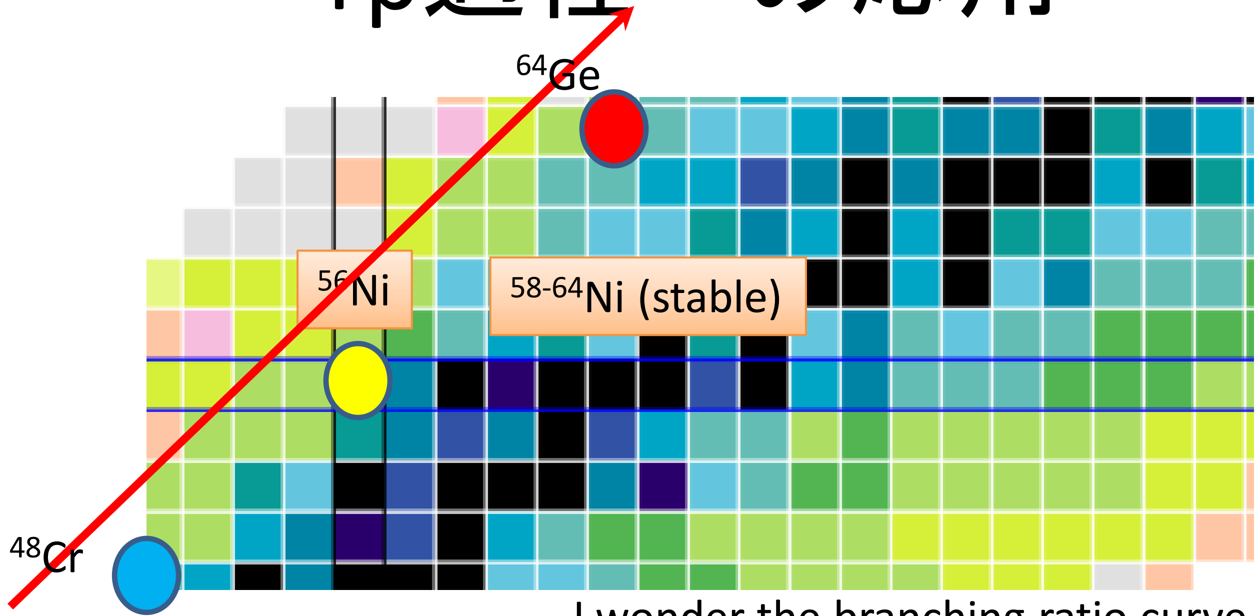

I wonder the branching ratio curve
(→ Γp/Γ(Ex)、Γ2p/Γ(Ex)、。。。)
obtained by the missing mass spsectroscopy
(not necessarily with (p,n))
is useful…

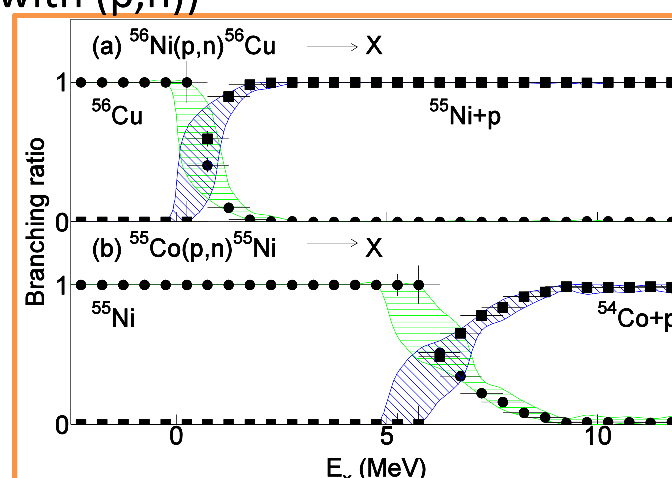

Beta+ decay : (n,p), (t,3He), …
→ Measuring mirror stable nuclei
(@RCNP、藤田さん)

N=Z→ 不安定核でB(GT) (@RIBF)

What is the key parameter in theoretical model?

まとめ

僕が重要だと思うこと

キーとなる原子核（二重閉殻核、興味のある宇宙物理現象で豊富な核）をはかる。
→背後にある物理を明らかにする（相互作用、配位混合、。。。。）
→　核モデルを向上
→　弱い相互作用反応率核モデルの予言能力を向上
＋　核モデル予言能力を評価する
（ここまでは原子核屋さんができる）

→　大規模な宇宙物理現象シミュレーションの予言能力を向上
＋　予言能力を評価する

以上のプロセスをさかのぼる。。。
→　核モデルの予言能力にたいする要求精度
→　どういった領域で、どういう精度でデータがほしいか？
→　核構造のどういった情報、物理をあきらかにすることが必要か？